Thermolysis and Photolysis of a γ-Azoperester. Cyclization of γ-Azo and γ-Perester Radicals

Paul S. Engel,*,† Shu Lin He,† and William B. Smith‡

Contribution from the Department of Chemistry, Rice University, 6100 Main Street, Houston, Texas 77005-1892, and Department of Chemistry, Texas Christian University, Fort Worth, Texas 76129

Received January 16, 1997[⊗]

Abstract: Thermolysis of azoperester **5** affords γ-azo radical **14**, which cyclizes to hydrazyl radical **15** at a rate of 1.3×10^9 M^{-1} s^{-1} at 110 °C. Our experimental results are consistent with loss of a methyl radical from **15** to afford 2-pyrazoline **9**, which is oxidized *in situ* by the starting **5** to pyrazole **6**. This unusual and endothermic β-scission can be rationalized if the odd electron in **15** is better aligned with the CH_3-C bond than with the weaker *t*-Bu−N bond. The fact that 5-endo cyclization of **14** is 5×10^7 faster than that of the analogous olefinic radical **30** led us to carry out *ab initio* calculations on simplified structures. $\Delta H^{\ddagger}$ for methyl radical addition to diimide is only 0.84 kcal/mol lower than for addition to ethylene and the exothermicity is only 3.5 kcal/mol greater. However, the smaller C−N═N than C−C═C bond angle leads to a $\Delta H^{\ddagger}$ 13.3 kcal/mol lower for 5-endo cyclization of 4,5-diazapenten-1-yl than for the analogous 4-pentenyl radical. Photolysis of **5** selectively cleaves the azo group, producing γ-perester radical **20**. This species undergoes intramolecular attack on the peroxide linkage to form lactone **23** at a rate of 1.5×10^4 s^{-1} at 22 °C. The cyclization rate of **20** is slow enough that **5** could be used as a photochemical bifunctional initiator, but cyclization of **14** to the azo group is so rapid that this radical would only rarely attack a monomer.

Introduction

Bifunctional free radical initiators contain two groups capable of forming radicals thermally or photochemically.[1] Before such initiators can be put to practical use, their chemistry in the absence of monomers must be understood. Moreover, study of these compounds can lead to fundamental knowledge about fragmentation and intramolecular reactions of radicals.

Azoperester **1** contains the two most common free radical initiators: an aliphatic azo group and a peroxy linkage.[2] Three years ago, we reported that long wavelength irradiation of **1** leads to a β-perester radical, **2**, which loses CO_2 at a rate k_β of 2.9×10^6 s^{-1} at 25 °C.[3] On the other hand, heating **1** to 110 °C caused initial homolysis of the perester moiety to yield a β-azo radical **3**,[4,5] which lost N_2 at a rate of about 2.5×10^9 s^{-1}.[6] These fragmentations are so fast that radicals **2** and **3** would rarely attack a monomer. In the present work we have studied azoperester **5**, a homolog of **1** that cannot undergo such multiple fragmentations. Photolysis of **5** produces a radical (**20**) that lives long enough to become a polymer end group, but thermolysis of **5** does not. This new bifunctional initiator was

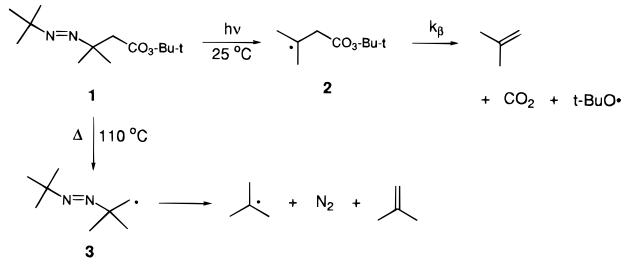

synthesized in 48% overall yield from acetone *tert*-butylhydrazone by the route shown below.[7]

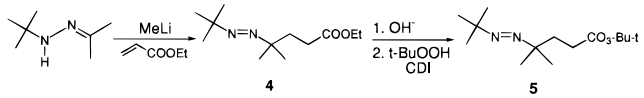

Thermolysis of 5. A degassed, sealed solution of **5** in benzene was thermolyzed at 110 °C for 1.5 h. NMR analysis showed that 95% of **5** had reacted while GC revealed six products, whose structures were tentatively assigned by GC/MS and then proven by isolation or by coinjection of authentic samples. The product yields (cf. Table 1) were quantified using experimentally determined response factors, except for **7**. Pyrazole **6** and azoether **7** were isolated by preparative TLC.

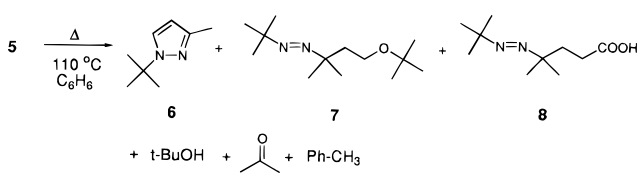

An authentic sample of **6** was prepared from butenone and *tert*-butylhydrazine,[8] followed by oxidation of the 2-pyrazoline **9**

† Rice University.

‡ Texas Christian University.

[⊗] Abstract published in *Advance ACS Abstracts,* June 1, 1997.

(1) Su, J. S. N.; Piirma, I. *J. Appl. Polym. Sci.* **1987**, *33*, 727. Comanita, E.; Popa, A. A. *Rev. Roum. Chim.* **1995**, *40*, 765. Gonzales, I. M.; Meira, G. R.; Oliva, H. M. *J. Appl. Poly. Sci.* **1996**, *59*, 1015. Narita, Y.; Kinoshita, H.; Araki, T. *J. Polym. Sci., Part A* **1992**, *30*, 333. Hepuzer, Y.; Bektas, M.; Denizligil, S.; Onen, A.; Yagci, Y. *J. Macromol. Sci., Pure Appl. Chem.* **1993**, *A30*, 111.

(2) Koenig, T. In *Free Radicals*; Kochi, J. K., Ed.; Wiley: New York, 1973; Vol. 1, Chapter 3. Moad, G.; Solomon, D. H. In *Comprehensive Polymer Science*; Allen, G. A., Bevington, J. C., Eds.; Pergamon Press: Oxford, 1989; Vol. 3, Chapter 8.

(3) Engel, P. S.; Wu, A.-Y. *J. Org. Chem.* **1994**, *59*, 3969.

(4) Engel, P. S.; Wang, C.-R.; Chen, Y.-Q.; Rüchardt, C.; Beckhaus, H.-D. *J. Am. Chem. Soc.* **1993**, *115*, 65.

(5) Engel, P. S.; Chen, Y.-C.; Wang, C. *J. Am. Chem. Soc.* **1991**, *113*, 4355.

(6) Wu, A.-Y. Ph.D. Dissertation, Rice University, 1994, p 65.

(7) Baldwin, J. E.; Adlington, R. M.; Bottaro, J. C.; Kohle, J. N.; Perry, M. W. D.; Jain, A. U. *Tetrahedron* **1986**, *42*, 4223.

(8) Auwers, K.; Brocha, H. *Chem. Ber.* **1922**, *55*, 3880. Elguero, J.; Jacquier, R.; Tarrago, G. *Bull. Soc. Chim. Fr.* **1966**, 293.

S0002-7863(97)00143-1 CCC: $14.00

Table 1. Products from Thermolysis of **5** in Benzene at 110 °C

compound	retn time,[a] min	response factor[b]	yield,[c] %	yield,[d] %
tert-butyl alcohol	2.44	0.74	53	91
acetone	2.32	0.49	46	0
toluene	5.69	1.07	22	0
pyrazole **6**	9.92	0.58	26	12
azoether **7**	13.89	0.79[e]	4.5	3.5
azoacid **8**	15.71	0.30	66	60

[a] DB-5 column, condition A (see the Experimental Section). [b] Relative to decane. [c] No added scavenger. [d] With 0.61 M *t*-BuSH. [e] Assumed to equal that of the ether from **1**.

with *tert*-butyl pervalerate **(10)**. Azoether **7** was identified by

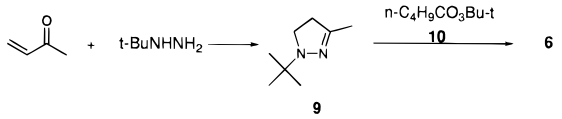

NMR and by CI/GC/MS, which has proven to be a powerful tool for structure determination of azoalkanes.[9] Whereas azo-*tert*-butane (ATB; the systematic name for this compound is 2,2′-azobis[2-methylpropane]) gave no molecular ion by EI, its CI/MS exhibited only three peaks of relative abundance greater than 5%, namely, protonated ATB, *m/e* = 143 (100), protonated *tert*-butyldiazene, *m/e* 87 (13), and *t*-Bu$^+$, *m/e* 57 (10). Likewise, every peak of **7** over 5% was easily rationalized, as shown below.

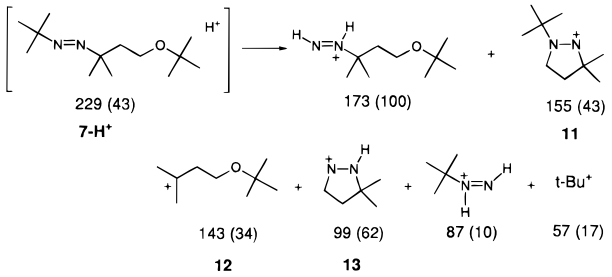

Origin of Pyrazole 6. This unusual product is postulated to arise by cyclization of **14** to hydrazyl radical **15**. Loss of methyl radical followed by perester oxidation of pyrazoline **9** affords **6**. To support this mechanism, the d_6 analog of **5** was

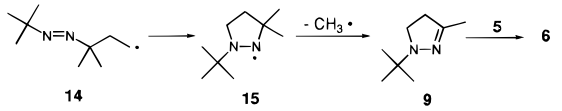

synthesized starting from acetone-d_6. Thermolysis was carried out exactly as with **5**, and the products were analyzed by GC/MS. The toluene peak contained 22% PhCD$_3$, strongly sug-

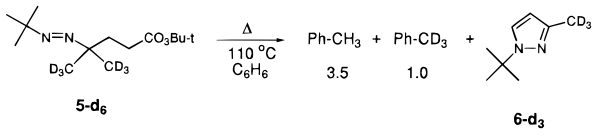

gesting that the cleaved $CD_3^\bullet$ group attacked the benzene solvent.[10] Fragmentation of the *tert*-butoxy group to acetone plus $CH_3^\bullet$ accounts for the PhCH$_3$. The pyrazole **6** was now found to be trideuterated, again consistent with the proposed mechanism. To confirm that **9** was an allowed reaction intermediate, the authentic compound was heated at 110 °C in benzene with model perester *tert*-butyl pervalerate (**10**). Under these conditions, pyrazoline **9** was converted to **6** while **10** was reduced to valeric acid. Heating **9** alone in benzene led to no reaction while heating **10** similarly led to no carboxylic acid. Thus, the high carboxylic acid yields from **5** (Table 1) are caused at least in part by perester oxidation of **9**.

Table 2. Methyl Radical Products of **5-*d*$_6$** in 1:1 Benzene−Nitrobenzene[a,b]

precursor	toluene (T)	*o*-nitro-T	*m*-nitro-T	*p*-nitro-T
di-*tert*-butyl hyponitrite	(1.00)	2.65	0.296	1.02
tert-butyl peracetate[c]	(1.00)	3.22	0.32	1.01
5-*d*$_6$	(1.00)	5.22	0.599	1.83
5-*d*$_6$ − ra ($ArCD_3/ArCH_3$)	0.079	0.12	*d*	0.11

[a] Samples thermolyzed at 110 °C. The first three rows are GC FID area ratios, and the last row is GC/CI/MS abundance ratios of D_3 to H_3 isotopes. For toluene the *m/e* 96 to *m/e* 93 ratio is listed while for nitrotoluenes the *m/e* 141 to *m/e* 138 ratio is listed. [b] AT-1701 column, GC condition A. [c] See ref. 12. [d] Not measured because the peak was too weak.

An alternate pathway to **6** is the oxidation of **15** to diazenium cation **16** followed by loss of CH_3^+.[11] We sought to distinguish

$CH_3^\bullet$ from CH_3^+ by thermolyzing **5** in a mixture of benzene and nitrobenzene. The methyl radical attacks nitrobenzene preferentially[12] while the cation should behave very much the opposite. To confirm the behavior of methyl radicals, a solution of *tert*-butyl hyponitrite[13] in 1:1 benzene−nitrobenzene was thermolyzed at 110 °C.[14] In accord with an earlier study,[12] nitrobenzene is at least 4 times more reactive than benzene, considering the presumably lower GC response factor of the nitrotoluenes than toluene (cf. Table 2). The analogous experiment with **5** required **5-*d*$_6$** to distinguish methyl groups arising from **15** from those of *tert*-butoxy radical β-scission. Again, the nitrotoluenes dominated over toluene (>7.6:1, Table 2), not the expected behavior of methyl cations. CI/GC/MS revealed that the relative yield of nitrotoluenes-d_3 was 10.5 times that of toluene-d_3 (0.12 × 5.22 + 0.11 × 1.83)/0.079. If the CD_3 groups from **5-*d*$_6$** turned up as CD_3^+, one would expect this figure to be far below unity. Furthermore, if much CD_3^+ were formed and were somehow able to methylate nitrobenzene, the percent meta from **5-*d*$_6$** should greatly exceed that from di-*tert*-butyl hyponitrite, but the actual figures were 7.8% and 7.5%, respectively (Table 2). Thus, the thermolysis of **5-*d*$_6$** in the mixed solvent does not yield methyl cations, contradicting the alternate mechanism.

Thermolysis kinetics of **5** and **10** were monitored by NMR, giving good first-order plots. The rate constants at 110 °C were 2.05×10^{-4} and 1.03×10^{-4} s^{-1}, respectively, showing that the bifunctional compound decomposed twice as fast as the simple perester. Interestingly, when an equimolar amount of **9** was included with **10**, the rate increased to 1.87×10^{-4} s^{-1}. We attribute the increase to oxidation of **9** by **10**, indicating that oxidation of **9** is also responsible for the faster thermolysis

(9) A CAS Online search of chemical ionization mass spec? gave 1616 hits, azo? gave 80385 hits, and the intersect of those sets gave only two hits, neither of which concerned aliphatic azo compounds.

(10) Levy, M.; Szwarc, M. *J. Am. Chem. Soc.* **1955**, *77*, 1949.

(11) If the starting azoperester serves as oxidizer both here and in the **9** → **6** conversion, this alternate mechanism would explain the 2.5-fold greater yield of **8** than **6**. However, we have seen high carboxylic acid yields from many bifunctional initiators.

(12) Pryor, W. A.; Davis, W. H.; Gleaton, J. H. *J. Org. Chem.* **1975**, *40*, 2099.

(13) Mendenhall, G. D. *Tetrahedron Lett.* **1983**, *24*, 451.

(14) Since the half-life is 12 s at this temperature,[15] most of the thermolysis took place below 110 °C.

(15) Kiefer, H.; Traylor, T. G. *Tetrahedron Lett.* **1966**, 6163.

Table 3. Product Yields[a] from Thermolysis[b] of 0.235 M **5** in the Presence of Tempo

[Tempo], M	**6**, %	**19**, %[c]	**7**, %	**8**, %
0.051	22.9	1.40	2.9	46.2[d]
0.231	13.9	3.71	2.4	76.1
0.282	14.2	4.16	2.3	77.1
0.359	10.9	4.39	2.0	80.7

[a] AT-1701 column, condition A. [b] Benzene at 110 °C. [c] Assumed response factor taken as the average of that for *t*-BuN=NCMe$_2$CH$_2$O-*t*-Bu (0.79) and *N*-*tert*-butoxy-2,2,6,6-tetramethylpiperidine (0.43). [d] DB-5 column.

rate of **5**. The reason why **5** thermolyzes twice as fast as **10** and appears first-order during the 1.5 half-lives that were monitored is that the second-order rate constant for oxidation of **9** is at least 100 times greater than that of the unimolecular thermolysis of **5**.[16]

Trapping of γ-Azo Radical 14. Thermolysis of **5** was expected to give γ-azo radical **14**, but attempts to trap this radical using *t*-BuSH did not produce detectable amounts of **18**, an authentic sample of which was synthesized independently. However, use of Tempo, a much faster radical trap,[17,18] led to a new GC peak at 18.2 min whose CI/GC/MS was beautifully consistent with structure **19**. (See the Experimental Section for

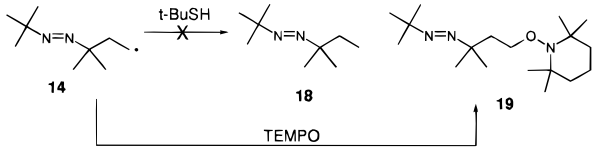

rationalization of all ions of relative abundance greater than 2%.) In order to estimate the lifetime of **14**, the yield of **6** and **19** was determined as a function of Tempo concentration (cf. Table 3). A plot of the yield of **19** over that of **6** versus [Tempo] was linear with a slope k_t/k_r of 1.09 where k_r is the rate constant of **14** → **15**. Because so little Tempo was consumed, we simply used its initial concentration in this plot. On the basis of the value $k_t = 1.4 \times 10^9$ M^{-1} s^{-1} for Tempo with primary radicals at 110 °C,[17,19] we obtain $k_r = 1.3 \times 10^9$ M^{-1} s^{-1}. Since trapping rates decrease at high concentrations of Tempo,[20] the proper graph[21] is ([**6**]/[**9**]) [Tempo] versus [Tempo]. In this case we obtained an intercept k_r/k_t of 0.83, corresponding to $k_r = 1.2 \times 10^9$ M^{-1} s^{-1}. The discrepancy between these numbers is much less than the uncertainty in the GC response factor of **19**, estimated to be ±20%.

In an attempt to trap **15-*d*$_6$**, a sample of **5-*d*$_6$** was thermolyzed in benzene at 110 °C with 0.494 M *t*-BuSH. GC analysis (AT-1701, condition A) revealed a new peak 1.24 min earlier than **6-*d*$_3$** and of very similar size. The CI mass spectrum of this peak was consistent with 1-*tert*-butyl-3,3-di(trideuteromethyl)-pyrazolidine (**17-*d*$_6$**), but the compound was neither isolated nor synthesized independently.

Photolysis of 5. Since 366 nm irradiation of **1** gave β-perester radical **2**, it was no surprise that similar treatment of **5** afforded γ-perester radical **20**. This species then underwent an intramolecular S_H2 reaction to yield lactone **23** in competition with disproportionation to peresters **21** and **22**. The only other

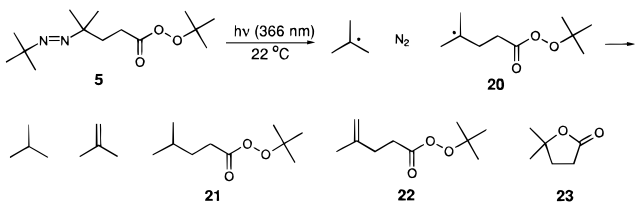

products detected were of low molecular weight: isobutene and isobutane from disproportionation, and acetone and *tert*-butyl alcohol from *t*-BuO•. The identity of **21**−**23** was proven by coinjection of authentic samples.

All of these products gave symmetrical, reproducible peaks on capillary GC (AT-1701 column). In the absence of a scavenger, the yields of isobutane, isobutene, **21**, and **22** were each in the region of 30%, suggesting that there is no selectivity in the disproportionation of the unsymmetrical radical pair *t*-Bu•/**20** (cf. Table 4). As 1,4-cyclohexadiene (CHD) was added, the yield of **21** rose, that of **23** fell, and **22** remained unchanged (cf. Table 5). These observations indicate that CHD does not interfere with the normal behavior of *t*-Bu•/**20** radical pairs, except to divert some of **20** to **21**. Although we previously[3] avoided using a H•-donating scavenger because the trapped product was identical to the cage product, we find here that the amount of **21** in excess of that produced by cage disproportionation is proportional to the CHD concentration. Thus, a plot of the yield ratio of (**21**−32%):**23** versus [CHD] (Table 5) was linear with slope $k_t/k_c = 0.618$ where k_c is the rate constant of **20** → **23**. The trapping rate k_t of *tert*-butyl radicals by CHD is 9.4×10^3 M^{-1} s^{-1} at 22 °C,[22] leading to $k_c = 1.5 \times 10^4$ s^{-1}.

Discussion

Thermolysis of aliphatic *tert*-butyl peresters normally yields an acycloxy radical plus a *tert*-butoxy radical.[23] Because decarboxylation is very rapid (for EtCOO•, $k = 2 \times 10^9$ at 20 °C),[24] the final products do not include the carboxylic acid. In the case of **5**, we have four unusual results: a high yield of acid **8**, an enhanced thermolysis rate relative to the model compound *tert*-butyl pervalerate (**10**), exceedingly fast 5-endo cyclization of β-azo radical **14**, and loss of CH_3• from pyrazolinyl radical **15**. The first two observations are readily explained by the facts that perester **10** indeed oxidizes **9** to **6**, that the disappearance rate of **10** is nearly doubled by inclusion of **9**, and that **9** increases the yield of valeric acid from 0 to 45%.

Intermolecular[25] and intramolecular[26,27] radical additions to the azo group are known, though these reactions are not nearly as common as addition to olefins.[28,29] On the other hand, 5-endo

(16) Kinetic modeling of the system A → B, A + B → C was carried out using the Chemical Kinetics Simulation package from IBM.

(17) Bowry, V. W.; Ingold, K. U. *J. Am. Chem. Soc*. **1992**, *114*, 4992.

(18) Newcomb, M. *Tetrahedron* **1993**, *49*, 1151.

(19) A solvent correction from isooctane to benzene reduces k_t by a factor of 0.61 while a temperature increase from 18 to 110°C raises k_t by a factor of 2.1.

(20) Hollis, R.; Hughes, L.; Bowry, V. W.; Ingold, K. U. *J. Org. Chem*. **1992**, *57*, 4284.

(21) Mendenhall, G. D.; Protasiewicz, J. D.; Brown, C. E.; Ingold, K. U. Lusztyk, J. *J. Am. Chem. Soc*. **1994**, *116*, 1718.

(22) Hawari, J. A.; Engel, P. S.; Griller, D. *Int. J. Chem. Kinet.* **1985**, *17*, 1215.

(23) Rüchardt, Ch. *Fort. Chem. Forsch.* **1966**, *6*, 251. Sawaki, Y. In *Organic Peroxides*; Ando, W., Ed.; Wiley: New York, 1993.

(24) Edge, D. J.; Kochi, J. K. *J. Am. Chem. Soc*. **1973**, *95*, 2635. Hilborn, J. W.; Pincock, J. A. *J. Am. Chem. Soc.* **1991**, *113*, 2683.

(25) Gray, P.; Thynne, J. C. J. *Trans. Faraday Soc*. **1963**, *59*, 2273. Dacey, J. R.; Mann, R. F.; Pritchard, G. O. *Can. J. Chem*. **1965**, *43*, 3215. Knoll, H.; Scherzer, K.; Geiseler, G. *Z. Phys. Chem.* **1972**, *249*, 359. Roberts, B. P.; Winter, J. N.; *Tetrahedron Lett*. **1979**, 3575. Strausz, O. P.; Berkley, R. E.; Gunning, H. E. *Can. J. Chem.* **1987**, *109*, 5289. Gorgenyi, M.; Kortvelyesi, T.; Seres, L. *J. Chem. Soc., Faraday Trans.* **1993**, *89*, 447.

(26) Benati, L.; Placucci, G.; Spagnolo, P.; Tundo, A.; Zanardi, G. *J. Chem. Soc., P1* **1977**, 1684. Leardini, R.; Nanni, D.; Tundo, A.; Zanardi, G. *J. Chem. Soc., Chem. Commun.* **1989**, 757. Alberti, A.; Bedogni, N.; Benaglia, M.; Leardini, R.; Nanni, D.; Pedulli, G. F.; Tundo, A.; Zanardi, G. *J. Org. Chem.* **1992**, *57*, 607. Leardini, R.; Lucarini, M.; Nanni, D.; Pedulli, G. F.; Tundo, A.; Zanardi, G. *J. Org. Chem*. **1993**, *8*, 2419. Christl, M.; Henneberger, H.; Freund, S. *Chem. Ber*. **1988**, 121, 1675.

(27) (a) Kunka, C. P. A.; Warkentin, J. *Can. J. Chem.* **1990**, *68*, 575. (b) Beckwith, A. L. J.; Wang, S.; Warkentin, J. *J. Am. Chem. Soc.* **1987**, *109*, 5289.

(28) Giese, B. *Angew. Chem., Int. Ed. Engl*. **1983**, *22*, 753.

Table 4. Products from Photolysis of **5** in Benzene at 22 °C

compound	retn time,[a] min	response factor[b]	yield, %
isobutane	1.44	1.0	29.6
isobutene	1.47	1.0	32.1
acetone	2.19	0.49	trace
tert-butyl alcohol	2.36	0.74	trace
21	19.45	0.36	32.0
22	21.27	0.33	28.2
23	13.20	0.55	34.7

[a] AT-1701 column, condition B (see the Experimental Section). [b] Relative to decane.

Table 5. Product Yields from Photolysis of **5** with 1,4-Cyclohexadiene[a,b]

[CHD], M	**21**	**22**	**23**
0.244	34.3	27.0	30.6
0.95	45.9	27.2	21.7
1.95	53.7	28.1	17.1
2.85	56.0	27.1	13.8

[a] 0.01 M **5** in benzene, 22 °C. [b] AT-1701 column, condition B.

cyclization is rare in olefins,[30,31] but cyclization to the azo group occurs in radicals **24** and **25** to give both 5-exo and 6-endo products.[27] 5- Endo cyclization of aryl radical **26** occurs at a

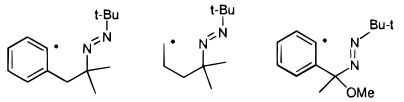

24 **25** **26**

rate of 9.2×10^8 s^{-1} at 80 °C while 5-exo cyclization of aryl radical **24** proceeds at 1.5×10^9 s^{-1} at 82 °C. Although no rate was stated for the analogous alkyl radical **25**, one can use the product ratios and the value 6.4×10^6 M^{-1} s^{-1} for Bu_3SnH trapping of primary alkyl at 80 °C[18] to calculate a 5-exo cyclization rate of 1.2×10^7 s^{-1} at 80 °C. This value is over 100 times slower than that for **24**, in accord with the higher reactivity of aryl radicals than alkyl. Although no directly comparable olefin cyclizations (e.g., *o*-allylphenyl vs 5-pentenyl radical) are known to help quantify further the reactivity of aryl versus alkyl radicals, **27** undergoes 5-exo cyclization 600 times faster than **28** at 110 °C and 2200 times faster at 25 °C.[32−34]

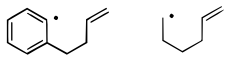

27 **28**

These comparisons suggest that 5-endo cyclization of an alkyl radical to the azo group should be hundreds of times slower than the 10^9 range seen for **26**; hence, it is remarkable that **14** undergoes exclusive 5-endo cyclization at a rate exceeding 10^9 s^{-1}. Beckwith et al.[30] found no cyclic products from **30**

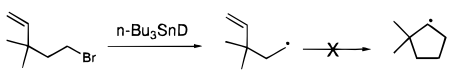

29 **30** **31**

Table 6. Calculated Enthalpies for Radical Addition

Reaction	$\Delta H^{\ddagger}$ [a,b]	ΔH_r [a,c]
$CH_3\bullet + C_2H_4 \longrightarrow CH_3CH_3CH_2\bullet$	8.49	-27.61
$CH_3\bullet + H_2N{-}NH \longrightarrow CH_3NHNH\bullet$	7.65	-31.17
	19.54	
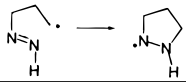	6.27	

[a] kcal/mol using UQCISD/6-31G*//UHF/6-31*. [b] Activation enthalpy. [c] Reaction exothermicity.

generated by Bu_3SnD reduction of **29**. If we assume a 1% detection limit and employ a value of 1.0×10^6 M^{-1} s^{-1} for n-Bu_3SnD with primary alkyl at 110 °C, the 5-endo cyclization rate of **30** would fall below 25 s^{-1}, which is 5×10^7 slower than that of the structurally analogous **14** → **15**.

The relatively large amount of 6-endo product from **24** has been attributed to an early transition state caused by resonance stabilization of hydrazyl radicals and to the shorter N═N bond and smaller C—N═N angle relative to olefins.[27] Which of these factors are responsible for the enormous rate enhancement of **14** versus the carbon analog **30**? The degree to which "hydrazyl resonance" accelerates cyclization of **14** might be evaluated if one knew the thermochemistry of simple intermolecular additions like methyl radical to ethylene and to diimide. Experimental values for the ethylene case are readily available, but the heats of formation (ΔH_f) of both diimide[35−37] and hydrazyl radicals[38−40] are not well established. Even if ΔH_f of hydrazyl itself were well known, it is possible that methyl substitution would stabilize this radical, similar to $MeNHCH_2^{\bullet}$ versus $H_2NCH_2^{\bullet}$.[41] The thermodynamic approach is the most direct way to compare olefins and azoalkanes; however, rotation barriers provide another estimate of the hydrazyl resonance energy. These barriers are about 8 kcal/mol in highly substituted hydrazyls while AM1-UHF calculations for $H_2N{-}NH^{\bullet}$ predict a barrier of 12.6 kcal/mol.[42]

Ab Initio Calculations of Radical Addition. To help understand the rapid cyclization rate of **14**, we calculated the enthalpy of activation ($\Delta H^{\ddagger}$) and the exothermicity (ΔH_r) of the two intermolecular and two intramolecular reactions shown in Table 6. Many theoretical treatments have dealt with the addition of radicals to olefins,[43] but the only calculation on azo compounds[44] was semiempirical and is seriously at odds with the ab initio results presented below. In their detailed studies of the addition of methyl and related radicals to a series of

(29) Walbiner, M.; Wu, J. Q.; Fischer, H. *Helv. Chim. Acta* **1995**, *78*, 910. Tedder, J. M.; Walton, J. C. *Tetrahedron* **1980**, *36*, 701. Tedder, J. M. *Angew. Chem., Int. Ed. Engl.* **1982**, *21*, 401, 433. Tedder, J. M.; Walton, J. C. *Acc. Chem. Res.* **1976**, *9*, 183.

(30) Beckwith A. L. J.; Easton, C. J.; Lawrence, T.; Serelis, A. K. *Aust. J. Chem.* **1983**, *36*, 545.

(31) Bogen, S.; Malacria, M. *J. Am. Chem. Soc.* **1996**, *118*, 3992.

(32) Beckwith, A. L. J.; Schiesser, C. H. *Tetrahedron* **1985**, *41*, 3925.

(33) Johnson, L. J.; Lusztyk, J.; Wayner, D. D. M.; Abeywickrema, A. N.; Beckwith, A. L. J., Scaiano, J. C., Lee, K. H.; Chin, K. L.; Brumby, S. *J. Am. Chem. Soc.* **1985**, *107*, 4594.

(34) Beckwith, A. L. J. *Landolt-Bornstein, New Series Vol. 13a, Radical Reaction Rates in Liquids*, Springer-Verlag: Berlin 1984; p 276.

(35) Engel, P. S.; Owens, W. H.; Wang, C.-R. *J. Phys. Chem.* **1993**, *97*, 10486.

(36) Foner, S. N.; Hudson, R. L. *J. Chem. Phys.* **1978**, *68*, 1.

(37) Ruscic, B.; Berkowitz, J. *J. Chem. Phys.* **1991**, *95*, 4378.

(38) Grela, M. A.; Colussi, A. J. *Int. J. Chem. Kinet.* **1988**, *20*, 713.

(39) Ingemann, S.; Fokkens, R. H.; Nibbering, N. M. M. *J. Org. Chem.* **1991**, *56*, 607.

(40) Foner, S. N.; Hudson, R. L. *J. Chem. Phys.* **1958**, *29*, 442.

(41) Griller, D.; Lossing, F. P. *J. Am. Chem. Soc.* **1981**, *103*, 1586. Theoretical calculations do not reproduce the alkyl group effect. Kysel, O.; Mach, P. *THEOCHEM* **1986**, *139*, 333.

(42) Nelsen, S. F. In *Acyclic Organonitrogen Stereodynamics*, Lambert, J. B., Takeuchi, Y., Eds.; VCH Publishers: New York, 1992; p 256.

(43) Basilevsky, M. V.; Chlenov, I. E. *Theor. Chim. Acta* **1969**, *15*, 174. Hoyland, J. R. *Theor. Chim. Acta* **1971**, *22*, 229. Fujimoto, H.; Yamabe, S.; Minato, T.; Fukui, K. *J. Am. Chem. Soc.* **1972**, *94*, 9205. Dewar, M. J. S.; Olivella, S. *J. Am. Chem. Soc.* **1978**, *100*, 5290. Clark, D. T.; Scanlan, I. W.; Walton, J. C. *Chem. Phys. Lett.* **1978**, *55*, 102. Fueno, T.; Kamachi, M. *Macromolecules* **1988**, *21*, 908. Gonzales, C.; Sosa, C.; Schlegel, H. B. *J. Phys. Chem.* **1989**, *93*, 2435, 8388. Zipse, H.; He, J.; Houk, K. N.; Giese, B. *J. Am. Chem. Soc.* **1991**, *113*, 4324. Wong, M. W.; Pross, A.; Radom, L. *J. Am. Chem. Soc.* **1993**, *115*, 11050. Wong, M. W.; Pross, A.; Radom, L. *Isr. J. Chem.* **1993**, *33*, 415. Wong, M. W.; Pross, A.; Radom, L. *J. Am. Chem. Soc.* **1994**, *116*, 6284.

(44) Kortvelyesi, T.; Seres, L. *React. Kinet. Catal. Lett.* **1995**, *56*, 371.

Table 7. Geometry of Transition States

Reaction	Bond Length, Å	Bond Angle, °	Torsion Angle, °
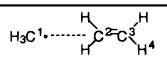	1,2 2.25 2,3 1.38	1-2-3 109.0	1-2-3-4 -87.0
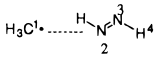	1,2 2.11 2,3 1.29	1-2-3 109.9	1-2-3-4 -77.9
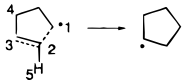	1,2 2.23 2,3 1.39	1-2-3 88.8 2-3-4 116.6	1-2-3-4 -41.8 1-4-3-2 37.3 5-2-3-4 -162.3
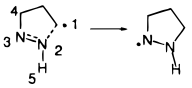	1,2 2.13 2,3 1.29	1-2-3 97.4 2-3-4 106.8	1-2-3-4 -44.5 1-4-3-2 37.4 5-2-3-4 -160.8

olefins, Wong and Radom[45] found that QCISD/6-31G* energies based on UHF/6-31G* geometries offered an adequate description of these reactions. As a test of our methodology, the transition structure (TS) for the addition of methyl radical to ethylene was calculated starting from their geometry (UQCISD/6-31G*//UHF/6-31G*). The resulting geometry and energy ($\Delta H^{\ddagger} = 8.49$ and $\Delta H_r = -27.61$ kcal/mol) were in exact agreement with those of Wong and Radom (cf. Tables 6 and 7).

The starting point for modeling the TS for the addition of the methyl radical to *trans*-diimide was the corresponding structure for ethylene. Initial calculations were carried out at the 3-21G* level; then cases of interest were reoptimized at the UHF/6-31G* level before energy determinations were made. In view of the possible interaction of the attacking methyl with the nitrogen lone pair electrons, a wide range of C−N−N−H torsion angles was explored as well as various attack angles (C−N−N). Several TSs were found by this procedure, indicating that the methyl−diimide potential energy surface is considerably more complex than for the methyl−ethylene system. However, the TS given in Table 7 was found to be significantly below all others and was taken as representing the optimum energy pathway for the reaction forming the 1-methyl-2-hydrazyl radical.

The calculated $\Delta H^{\ddagger}$ for methyl plus diimide is about 0.8 kcal/mol below that for methyl plus ethylene, and the ΔH_r is 3.5 kcal/mol more exothermic. These small differences and therefore "hydrazyl resonance" cannot account for the observed rate acceleration of **14** versus **30**. The transition state geometries (Table 7) show that the attack angle (1−2−3) is nearly identical for ethylene and diimide but the torsion angle is about 9° smaller for diimide. This deviation from perpendicular could be simply due to steric interaction between $CH_3^{\bullet}$ and the hydrogen on the N being attacked.

The TS for the cyclization of 4-penten-1-yl was initiated using the C−C bond lengths found for the ethylene case while the corresponding cyclization of the 4,5-diaza-4-penten-1-yl radical was modeled upon the TS for the all-carbon analog. The calculated difference in $\Delta H^{\ddagger}$ for 4-pentenyl versus the diaza analog (Table 6) is 19.54−6.27 = 13.27 kcal/mol, corresponding to a slower cyclization of 4-pentenyl by a factor of 3.7×10^7 at 110 °C. Since our observed rate for **14** is 1.2×10^9 s^{-1}, the estimated rate for **30** is 32 s^{-1}, an expectedly slow value. We have assumed that the rate enhancement due to the Thorpe Ingold effect is reflected only in $\Delta H^{\ddagger}$ and is the same for the hydrocarbon and diaza systems. On the basis of the data for radical cyclization to olefins,[18] the first assumption appears quite good. The self-consistency of this calculation suggests that unlike the 2-formylbenzoyl radical,[21] the rate-limiting step is radical cyclization, not rotation of **14** into the proper conformation.

(45) Wong, M. W.; Radom, L. *J. Phys. Chem.* **1995**, *99*, 8582.

In accord with the thermochemistry (Table 6), the calculated TS geometries (Table 7) show that bond making is slightly more advanced in the diazapentenyl than the hydrocarbon analog, judging from its shorter 1,2-bond distance and the greater deviation of its 5−2−3−4 torsion angle from 180°. A molecular model of the 5-pentenyl TS reveals a great deal of strain if the radical attacks perpendicular to the nodal plane of the double bond and at the ideal 1−2−3 angle of 109°.[32] These requirements are compromised in the actual TS, where the 1−2−3 angle is 88.8° and the 1−2−3−4 torsion angle is 41.8°. To rationalize the facile cyclization of diazapentenyl (Table 6), one can say simply that the azo group is more tolerant of nonideal attack angles than an olefin, but we did not investigate the possibility computationally. Alternately, one can recognize, as did earlier workers[27b] that the C−N═N angle of azoalkanes is about 10° smaller and the double bond is about 0.1 Å shorter[46] than in olefins. Reducing the 2−3−4 angle has two beneficial effects: it moves the carbon radical farther behind the site of attack, closer to the ideal 109°, (∠1−2−3 = 97.4°), and it increases the 1−2−3−4 torsion angle to 44.4°, placing the attacking radical farther above the 2,3,4 plane than in the 5-pentenyl radical. As reflected in the activation energies (Table 6), far less strain is encountered to achieve this acceptable geometry in the diaza than in the hydrocarbon case. To estimate the increase in ring strain during cyclization, each acyclic radical was first minimized as a linear zigzag structure using the MMX force field of PCMODEL (Mac version 4.51, Serena Software, Bloomington, IN). The difference in strain energy was 1.1 kcal/mol, favoring the diaza radical. Minimization of the cyclization TSs was then carried out with a fixed 1−2 atom distance (see atom numbering in Table 7). The diazapentenyl TS was now 5.0 kcal/mol below that of the hydrocarbon radical, offering a partial explanation for the cyclization rate enhancement. An additional but minor contribution may arise from the absence of a syn hydrogen on the azo nitrogen being attacked, on the basis of the observations that a 5-methyl group slows 5-endo cyclization of 5-hexenyl radical by a factor of 40[32] and that hydrogen−methyl repulsion in diimide reduces the torsion angle during attack (−77.9°, Table 7).

An additional result of our calculations is the N−H bond dissociation energy (BDE) of methylhydrazine, 75.0 kcal/mol (cf. Table 8). This figure can be compared with the experimental N−H BDE for hydrazine itself (80.5 kcal/mol[47]) and with a recently determined BDE for hydrazobenzene (73.1 kcal/mol).[39]

FMO theory has been widely discussed for free radical addition to olefins,[28,48] but is unable to rationalize the results in Table 6. The SOMO of a primary radical (IP = 8.7 eV)[49] is closer to the LUMO (π^*) orbital of ATB (EA = 0.63 eV)[50] than to the π^* orbital of propene (EA = 1.99 eV),[51] and the smaller SOMO−LUMO energy gap would predict faster radical attack on the azo linkage. While this notion is consistent with

(46) Experimental olefin and azoalkane bond lengths and angles are 1.34 Å, 124.3° and 1.254 Å, 111.9°, respectively, while the calculated values (UQCISD/6-31G*, cf. Supporting Information for output files) for 5-pentenyl and the diaza analog case are 1.32 Å, 125.35° and 1.22 Å, 115.35°, respectively.

(47) This is the most recent N−H BDE of hydrazine. An earlier experimental value (76 kcal/mol) and estimated value (87.5 kcal/mol) can be found in refs 40 and 38, respectively.

(48) Fleming, I. *Frontier Orbitals and Organic Chemical Reactions*; Wiley: London, 1976; p 182.

(49) Traven, V. F. *Frontier Orbitals and Properties of Organic Molecules;* Ellis Horwood, Ltd.: West Sussex, 1992; p 295.

(50) Modelli, A.; Jones, D.; Rossini, S.; Distefano, G. *Tetrahedron* **1984**, *40*, 3257.

(51) Franklin J. L.; Dillard, J. G.; Rosenstock, H. M.; Herron, J. T.; Draxl, K. *Ionization Potentials, Appearance Potentials, and Heats of Formation of Gaseous Positive Ions*; NSRDS-NBS 26; U.S. Government Printing Office: Washington, DC, 1969.

Table 8. UQCISD/6-31G* Energies Based on UHF/6-31G* Geometries

species	energy, hartrees	species	energy, hartrees
methyl radical	−39.688 868 5	1-methyl-2-hydrazyl radical	−150.071 561 9
ethylene	−78.312 405 2	4-penten-1-yl radical	−195.188 837 6
propyl radical	−118.045 267 4	4-penten-1-yl TS	−195.157 692 5
methyl−ethylene TS	−117.987 738 4	4,5-diazapenten-1-yl radical	−227.204 953 7
cis-diimide	−110.323 098 7	4,5-diazapenten-1-yl TS	−227.194 960 2
trans-diimide	−110.333 014 7	methylhydrazine	−150.689 353 5
methyl−*trans*-diimide TS	−150.009 697 6	hydrogen atom	−0.498 232 9

the rapid cyclization of **14**, the ab initio results show only a 0.84 kcal/mol $\Delta H^{\ddagger}$ difference between diimide and ethylene (Table 6). Radical attack on the azo n$_-$ orbital (IP = 8.2 eV) appears to be a good energetic match, but the third electron would have to go into a high-lying σ^* orbital.

Fragmentation of Hydrazyl Radical 15. Our results indicate that hydrazyl **15** undergoes an unusual C−C homolysis, resulting in loss of a methyl radical. C−N homolysis of hydrazyl radicals is known in such compounds as **32**[52] and **33**,[53] but **34** does not lose *tert*-butyl• because the odd electron is in a

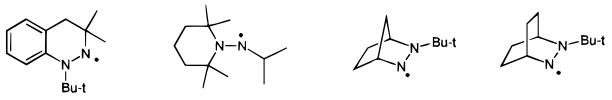

32 **33** **34** **35**

p orbital perpendicular to the C−N bond to be cleaved.[54] The same situation must obtain for **15**. Even though loss of *t*-Bu• would be thermodynamically favored over loss of CH_3•, the five-membered ring prevents the necessary torsion about the N−N bond that would allow overlap of the odd electron p orbital with the N−*t*-Bu bond. On the other hand, the CH_3−C bond of **15** is sufficiently well aligned to exhibit the first case of hydrazyl C−C homolysis. In **32**, the flexibility of the six-membered ring permits the requisite overlap so only the thermodynamic process takes place, despite the loss of hydrazyl resonance in the transition state.[55] Although the C_α−C_β bond of bicyclic hydrazyl **35** is well aligned with the nitrogen p orbital for β-scission, this radical actually persists for months.[54] The greater entropy for fragmentation of **15** than **35** and the high temperature of our study apparently facilitate β-scission of **15**.

To enhance our understanding of hydrazyl fragmentation, we calculated the enthalpy change of a simple model reaction. MP2 calculations on species **36**−**38** gave total energies of

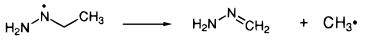

36 **37** **38**

−189.208 641, −149.481 871 8, and −39.670 749 9 hartrees, respectively. Fragmentation of **36** is therefore endothermic by 35.2 kcal/mol. If we neglect the barrier to the reverse reaction and use the highest reasonable log *A* value (17)[56] in the Arrhenius equation, the half-life of **36** comes out to be 32 min at 110 °C. Fragmentation of **15** should be more favorable than that of **36** on account of the fully substituted C=N bond in **9**. However, this large endothermicity and our tentative success in trapping **15** suggest that fragmentation occurs only when no other pathway is available. Independent generation and study of **15** would be a worthwhile endeavor.

Cyclization of γ-Perester Radical 20. While γ-azo radical **14** cyclizes very rapidly, the related γ-perester radical **20** affords lactone **23** much more slowly. The attack of radicals on the peroxy bond is well known, and its synthetic possibilities have been explored recently.[57] Using the reaction of **39** with CCl_4

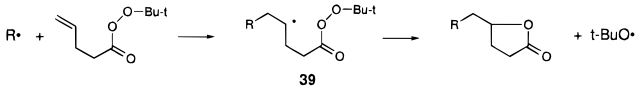

39

as a radical clock, Maillard and co-workers obtained a cyclization rate constant of 4×10^4 s^{-1} at 80 °C.[58] Despite the lower temperature and the tertiary nature of the attacking radical in **20**, our measured k_c of 1.5×10^4 s^{-1} at 22 °C is slower than this value by only a factor of 2.6. It appears from these results that more methyl groups on the attacking radical center have little effect on the lactonization rate, much like the 5-hexenyl radical.[18]

In connection with our interest in bifunctional free radical initiators,[1] it is useful to compare the k_c of **20** with the β-scission rate of **2**, where k_β/k_r of a cyclopropyl analog was 0.16. The

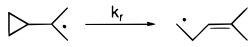

most recent value[59] of k_r is 1.8×10^7 s^{-1}, so that k_β is 2.9×10^6 s^{-1} at 25 °C. Since cyclization of **20** is 200 times slower than β-scission of **2**, irradiation of **5** should produce tertiary radicals that initiate sytrene polymerization much faster than they cyclize. The addition rate of **20** to styrene is 1.3×10^5 M^{-1} s^{-1} × 8.7 M = 1.1×10^6 s^{-1},[1] which is 73 times faster than cyclization of **20**. While 34% of **2** would be incorporated into polystyrene, the figure is nearly 99% for **20**. Production of an initiator-containing polymer from **5** by photochemical initiation is therefore feasible, but due to the rapid cyclization of **14**, thermal initiation is not. To achieve that goal, the azo and perester groups will have to be separated by a rigid spacer.

In summary, we have found that γ-azo radical **14** produced by thermolysis of **5** cyclizes at least 5×10^7 faster than the analogous olefinic radical **30**. *Ab initio* calculations of the 4,5-diazapenten-1-yl radical, methyl plus diimide, and the related olefins suggest that the normally "forbidden" 5-endo cyclization is facilitated by the smaller C−N=N than C−C=C angle. We propose that following cyclization, hydrazyl radical **15** undergoes an unprecedented cleavage of a methyl radical to afford a pyrazoline **9** which is finally oxidized by the starting perester to pyrazole **6**. Since the azo chromophore absorbs at much longer wavelength than the perester, near UV irradiation of **5** produces γ-perester radical **20** which cyclizes to lactone **23** at a rate of 1.5×10^4 s^{-1} at 22 °C. This reaction is slow enough that **5** could be used as a bifunctional radical initiator. However, thermolysis of **5** would not produce an azo-containing polymer because cyclization of **14** is too rapid.

(52) Wang, S. F.; Mathew, L.; Warkentin, J. *J. Am. Chem. Soc.* **1988**, *110*, 7235.
(53) Kaba, R. A.; Lunazzi, L.; Lindsay, D.; Ingold, K. U. *J. Am. Chem. Soc.* **1975**, *97*, 6762.
(54) Nelsen, S. F.; Landis, R. T. *J. Am. Chem. Soc.* **1973**, *95*, 6454.
(55) Raban, M.; Aviram, K.; Kost, D. *Tetrahedron Lett.* **1985**, *26*, 3591.
(56) Benson, S. W.; O'Neal, H. E. *Kinetic Data on Gas Phase Unimolecular Reactions*; NSRDS-NBS-21; U.S. Government Printing Office: Washington, D.C., 1970; p 28.
(57) Degueil-Castaing, M.; Navarro, C.; Ramon, F.; Maillard, B. *Aust. J. Chem.* **1995**, *48*, 233. Ramon, F.; Degueilcastaing, M.; Maillard, B. *J. Org. Chem.* **1996**, *61*, 2071.
(58) Maillard, B.; Kharrat, A.; Gardrat, C. *Nouv. J. Chim.* **1987**, *11*, 7.
(59) Engel, P. S.; He, S.-L.; Banks, J. T.; Ingold, K. U.; Lusztyk, J. *J. Org. Chem.* **1997**, *62*, 1210.

Experimental Section

Instrumentation. NMR spectroscopy: Bruker AC-250 with δ relative to $CDCl_3$ (7.26), C_6D_6 (7.15) or TMS (0.00). All ^{1}H NMR spectra were obtained at 250 MHz and all ^{13}C spectra at 62.5 MHz in $CDCl_3$ unless otherwise specified. IR spectroscopy: Nicolet 205 FT-IR. Mass spectrometry: Finnigan MAT 95. CI spectra employed methane as reactant gas. UV spectroscopy: HP8452A diode array spectrometer. Analytical GC: HP5890A with a DB-5 capillary column (0.25 mm × 30 m) or a AT-1701 capillary column (0.25 mm × 30 m) and HP3365 software. GC condition A: injector 210 °C, detector 250 °C, initial temperature 35 °C, initial time 2.5 min, 10 °C /min ramp to 250 °C. GC condition B: injector 170 °C, detector 250 °C, initial temperature 35 °C, initial time 2.5 min, 10 °C/min ramp to 100 °C, hold for 15 min, then ramp to 170 °C at 10 °C/min, final time 10 min.

Materials. Ether and THF were distilled from Na/Ph_2CO, while hexane was distilled from sodium. Benzene and methylene chloride were distilled from CaH_2. Decane, used as a GC internal standard, and 1,4-cyclohexadiene, used as a scavenger, were distilled before use. Tempo was purified by column chromatography and sublimation. All other starting materials were used as received.

Thermolysis and Photolysis Techniques. All samples for rate and product studies were freeze−thaw−degassed (−196 °C) three times and sealed on a vacuum line. For thermolysis, the tubes were immersed completely in a DC-200 silicone oil bath contained in a 1.5 gal Dewar flask with a mechanical stirrer. The temperature was regulated by a Bayley Model 123 temperature controller and was measured with a Hewlett-Packard Model 3456A digital voltmeter and a platinum thermometer. An Oriel 500 W high-pressure mercury lamp with a 366 nm filter solution was employed in photolysis work.

The thermolysis of di-*tert*-butyl hyponitrite and **5-*d*$_6$** in benzene−nitrobenzene is a typical GC experiment**.** A 9 mg portion of di-*tert*-butyl hyponitrite[13] in 0.6 mL of a 1:1 v/v solution of benzene and nitrobenzene was degassed and sealed into a 7 mm × 6 cm Pyrex tube. After heating at 110 °C for 15 min, the tube was opened and the contents were analyzed on the AT-1701 capillary column using GC condition A described under Instrumentation. Toluene, *o*-nitrotoluene, and *p*-nitrotoluene were identified by coinjection with authentic samples while the small peak at 15.35 min was assumed to be *m*-nitrotoluene on the basis of boiling points (ortho 221.7 °C, meta 232.6 °C, and para 238.3 °C) and expected product ratios (cf. Table 2). Other GC peaks of size similar to these were observed but were not assigned. A 0.066 M solution of **5-*d*$_6$** in the same solvent mixture was thermolyzed at 110 °C for 1.5 h and then analyzed by GC and by CI/GC/MS. Because the deuterated compounds exhibited a shorter retention time than the protiated compounds, the mass spectrum was summed over the GC peak due to both species.

CI Mass Spectrometry. Tempo trapping product **19** was identified only by this technique, giving ions at *m/e* (relative abundance) assignment 311 (4) $M^{\bullet+}$, 312 (5) MH^+, 296 (3) $M^+ - CH_3^{\bullet}$, 226 (3) MH^+ − *t*-BuNNH analogous to **12**, 155 (100) **11**, 140 (22) 2,2,6,6-tetramethylpiperidinium cation, and 99 (6) 3,3-dimethylpyrazolidinium cation **13**. The assignment of the tempo-derived fragments was supported by the CI/MS of 1-methoxy-2,2,6,6-tetramethylpiperidine:[60] *m/e* 172 (25) MH^+, 171 (40) $M^{\bullet+}$, 170 (22) $M^{\bullet+} - H^{\bullet}$, 156 (41) $M^{\bullet+} - CH_3^{\bullet}$, 140 (100) 2,2,6,6-tetramethylpiperidinium cation, 126 (7) $M^{+\bullet} - CH_3 - CH_2O$. The tentative structural assignment of **17-*d*$_6$** is based only on CI/GC/MS: *m/e* 163 (8) MH^+, 162 (15) $M^{\bullet+}$, 147 (68) $M^{\bullet+} - CH_3$, 131 (32), 119 (56) $M^{+\bullet} - CH_3 - C_2H_4$, 107 (93) MH^+ − isobutene, 57 (100) *t*-Bu^+.

Theoretical Calculations. Ab initio geometry optimizations were carried out at the UHF/6-31G* level either with SPARTAN[61] or with Gaussian 94.[62] A ll transition structures met the requirement of one imaginary frequency corresponding to the reaction coordinate.

Ethyl 4-Methyl-4-(*tert*-butylazo)pentanoate (4). Even though methyl acrylate was said to give negligible yields of C-addition products with acetone *tert*-butyl hydrazone (ATBH) anion,[7] we experienced no difficulty preparing **4**. ATBH was synthesized in 90% yield according to the literature.[63] ^{1}H-NMR: δ 1.17 (s, 9H), 1.71 (s, 3H), 1.92 (s, 3H). To a solution of ATBH (1.28 g, 10 mmol) in THF (40 mL) at −20 °C was added MeLi (8 mL, 11.2 mmol, 1.4 M in hexane). The solution was stirred for 30 min at −20 °C and then cooled to −60 °C. A solution of ethyl acrylate (1.3 g, 13 mmol) in THF (10 mL) was added, and the color of the solution changed from orange to light yellow. After stirring for 2 h at −60 °C, acetic acid (1 mL) in hexane (20 mL) was added and the mixture was slowly warmed to room temperature. Water (30 mL) was added, and the organic layer was separated. The aqueous layer was extracted with ether (2 × 30 mL). The combined organic solution was dried over $MgSO_4$ and filtered, and the solvent was rotary evaporated. The product **4** (1.6 g, 70%) was obtained by flash column chromatography on silica gel (ethyl acetate−hexane, 1:8). ^{1}H NMR: δ 1.09 (s, 6H), 1.14 (s, 9H), 1.24 (t, 3H, J = 7.1 Hz), 1.99 (m, 2H), 2.25 (m, 2H), 4.11 (q, 2H, J = 7.1 Hz). ^{13}C NMR: δ 12.17, 22.64, 25.11, 27.74, 33.94, 59.73, 66.79, 67.01, 177.1.

4-Methyl-4-(*tert*-butylazo)pentanoic Acid (8). NaOH (aqueous 20%, 4 mL) was added to a solution of **4** (1.14 g, 5 mmol) in 30 mL of ethanol at room temperature. The reaction mixture was stirred for 4 h. Ethanol was rotary evaporated, and the residue was dissolved in 10 mL of water. The aqueous solution was washed with ether (30 mL) and acidified with aqueous HCl to pH 2. This acidic solution was extracted with ether (3 × 50 mL). The combined ether layers were dried over $MgSO_4$. After filtration and solvent evaporation, **8** was obtained as a solid (940 mg, 94%), mp 31−32 °C. ^{1}H NMR: δ 1.10 (s, 6H), 1.15 (s, 9H), 1.99 (m, 2H), 2.33 (m, 2H). ^{13}C NMR: δ 24.38, 26.70, 29.10, 34.96, 66.90, 67.05, 180.20. MS (M + 1): *m/e* 201 (100), 183 (10). Anal. Calcd: C, 59.97; H, 10.06; N, 13.99. Found: C, 60.04; H, 9.89; N, 14.11.

***tert*-Butyl 4-Methyl-4-(*tert*-butylazo)peroxypentanoate (5).** Using the method of Staab et al.,[64] a solution of **8** (710 mg, 3.55 mmol) in THF (5 mL) was added to a solution of 1,1′-carbonyldiimidazole (737 mg, 4.5 mmol) in 10 mL of THF at room temperature, and the reaction mixture was stirred for 0.5 h. *tert*-Butyl hydroperoxide (410 mg, 5.5 mmol) was added at 0 °C, and the reaction was stirred for 4 h. Ether (25 mL) was added, and this solution was washed with aqueous NaOH (5%), water, and brine. The ether solution was dried over Na_2SO_4. After filtration and evaporation of solvent, the residue was chromatographed on Florisil (ethyl acetate−hexane 1:15). A yield of 620 mg of **5** (64%) was obtained. ^{1}H NMR (C_6D_6): δ 0.99 (s, 6H), 1.12 (s, 9H), 1.15 (s, 9H), 2.05 (m, 2H), 2.15 (m, 2H). ^{13}C NMR: δ 24.37 (Me_2), 26.14 (*t*-Bu), 26.27 (CH_2), 26.75 (*t*-Bu), 35.17 (CH_2), 66.51 (C), 67.00 (C), 83.30 (C), 171.3 (CO). IR (neat): 2975, 1779 cm^{-1}. UV (hexane): 366 nm (ϵ 22). The methylene peaks of **5** were unexpectedly complex.[65]

Acknowledgment. We thank the National Science Foundation and the Robert A. Welch Foundation for financial support and Professors Stephen F. Nelsen, University of Wisconsin, and Thomas A. Albright, University of Houston, for helpful discussion. The critical and constructive comments of the reviewers are gratefully acknowledged.

Supporting Information Available: Synthesis and spectral data of **6**, **7**, **9**, **10**, **18**, **21**, **22**, and **23**, and a table of Gaussian 94 quantum chemical results (11 pages). See any current masthead page for ordering and Internet access instructions.

JA970143U

(60) Whitesides, G. M.; Newirth, T. L. *J. Org. Chem.* **1975**, *40*, 3448. The EI MS of this methyl trapping product exhibits *m/e* 171 (10.5) and 156 (100) and smaller *m/e* of ra below 18, but not *m/e* 140.

(61) Wavefunction, Inc., 18401 Von Karman Ave., Irvine, CA.

(62) Gaussian 94, Revision B.2: Frisch, M. J.; Trucks, G. W.; Schlegel, H. B.; Gill, P. M. W.; Johnson, B. G.; Robb, M. A.; Cheeseman, J. R.; Keith, T.; Petersson, G. A.; Montgomery, J. A.; Raghavachari, K.; Al-Laham, M. A.; Zakrzewski, V. G.; Ortiz, J. V.; Foresman, J. B.; Peng, C. Y.; Ayala, P. Y.; Chen, W.; Wong, M. W.; Andres, J. L.; Replogle, E. S.;. Gomperts, R.; Martin, R. L.; Fox, D. J.; Binkley, J. S.; Defrees, D. J.; Baker, J.; Stewart, J. P.; Head-Gordon, M.; Gonzalez, C.; Pople, J. A., Gaussian, Inc., Pittsburgh, PA, 1995.

(63) Smith, P. A. S.; Clegg, J. M.; Lakritz, J. *J. Org. Chem.* **1958**, *23*, 1595.

(64) Staab, H. A.; Rohr, W.; Graf, F. *Chem. Ber*. **1965**, *98*, 1122.

(65) While the spectrum of **5** was the most second-order, the methylenes of **4** and **8** (but not **7**) also appeared distorted. The reason is that conformationally mobile molecules ZCH_2CH_2Y are actually AA′XX′ systems that sometimes appear as A_2X_2. See: McLean, D.; Waugh, J. S. *J. Chem. Phys.* **1957**, *27*, 968. Silverstein, R. M.; LaLonde, R. T. *J. Chem. Educ*. **1980**, *57*, 343. We thank Dr. Lawrence B. Alemany for helpful discussion on this point.